Applied Geochemistry 159 (2023) 105838

Contents lists available at ScienceDirect

Applied Geochemistry

journal homepage: www.elsevier.com/locate/apgeochem

Porewater composition in clay rocks explored by advective displacement and squeezing experiments

M. Kiczka [a,*], P. Wersin [a], M. Mazurek [a], C. Zwahlen [a], A. Jenni [a], U. Mäder [b], D. Traber [c]

[a] Institute of Geological Sciences, University of Bern, Baltzerstrasse 1–3, CH-3012 Bern, Switzerland
[b] Rock-Water Consulting, Oberfeldstrasse 19, CH-3067 Boll, Switzerland
[c] Nagra, Hardstrasse 73, 5430 Wettingen, Switzerland

ARTICLE INFO

Editorial handling by: Mieke De Craen

ABSTRACT

Argillaceous rocks are foreseen in many countries as the potential hosts for nuclear waste repositories. The knowledge of the chemical composition of the free porewater in these formations is required for the understanding of the paleo-hydrogeological evolution, for the assessment of radionuclide solubilities and migration parameters and for assessing the long-term stability of the technical barrier system. High pressure squeezing and advective displacement are two methods that aim at direct sampling of this porewater fraction while minimizing experimental artefacts. Within the framework of a recent deep drilling campaign in Switzerland, targeting the Opalinus Clay as the designated host rock, a substantial dataset of porewater compositions was obtained by these two methods. It included 51 squeezing and 30 advective displacement experiments on drillcore samples from the Opalinus Clay and confining units distributed over 8 boreholes in 3 study areas. Porewater compositions obtained by either method reflect the geochemical characteristics of each siting region, such as different salinities and water types as well as depth gradients informing on the diffusive exchange with bounding aquifers. An in depth comparison of the Opalinus Clay porewater compositions obtained by both methods shows a high degree of consistency with regard to the ion ratios or mineral equilibria. The pH/pCO_2 system was found to be prone to experimental artefacts, but applying a correction, a fairly consistent dataset was obtained. Porewaters acquired by squeezing exhibit systematically lower salinities by 10–40% when compared to those from advective displacement. It is concluded that this is due to the mobilization of a higher fraction of an anion depleted porewater, either due to the higher mobilization of water from the diffuse layer or due to the expulsion of water from interlayer (-like) pores. The comparison with a geochemical model indicates that the experimental data from both methods can be considered as proxies for in-situ major-ion porewater compositions. It also confirms the robustness of the geochemical model predicting porewaters of the Opalinus Clay and confining units. Differences between in-situ, sample storage and extraction temperatures need to be taken into account when interpreting the porewaters obtained by either method and modelling in-situ porewater compositions. Combining different laboratory and analytical methods for porewater investigations in clay rocks provides an added value as it enables a detailed assessment of natural heterogeneities and experimental uncertainties.

1. Introduction

Argillaceous rocks are foreseen in many countries as the potential hosts for nuclear waste repositories (Altmann et al., 2012), due to their generally low permeability, favourable radionuclide retention properties and high self-sealing capability (Horseman et al., 1996). These properties, unfortunately, render the characterization of porewater geochemistry and transport properties difficult and time-consuming, as the porewater is not easily accessible for direct analysis (e.g. Pearson et al., 2003). The porewater composition and transport properties in clay-rich rocks are further affected by the negatively charged surfaces of the clay minerals. The repulsion of anions from the negatively charged clay surface leads to an anion exclusion effect in a part of the porosity and this can be described with a diffuse double layer (Sposito, 2004) or Donnan (Gimmi and Alt-Epping, 2018) approach. In principle, both approaches distinguish two porosity domains, containing an anion-depleted porewater and a charge balanced porewater, termed free porewater in the following. The two domains are at thermodynamic

* Corresponding author.
E-mail address: mirjam.kiczka@unibe.ch (M. Kiczka).

https://doi.org/10.1016/j.apgeochem.2023.105838
Received 17 February 2023; Received in revised form 20 August 2023; Accepted 8 November 2023
Available online 14 November 2023

equilibrium with species having equal potentials. The free porewater is considered to be additionally governed by mineral equilibria (Pearson, 1999). Thus, the free porewater composition is key to understanding the local porewater chemistry with respect to its hydrogeochemical evolution and spatial variability. It is further required for the investigation of the fate of radionuclides ultimately released by the waste or of the evolution of materials in the repository environment either by well-designed experiments or geochemical modelling. Given the complexity of the a priori unknown porosity distribution (see also Zwahlen et al., 2023) classical methods targeting the bulk porewater composition such as aqueous extraction do not directly provide the anion concentrations in the free porewater. The interpretation of reactive components including sulphate (Aschwanden et al., 2023b), inorganic carbon or cation compositions, in those experiments is further complicated by the presence of large reactive mineral surface areas, including the clay exchanger. Good estimates of free porewater compositions in clay rocks have however been obtained by the combination of different experimental approaches (aqueous extraction, cation exchange experiments, water content measurements, mineralogy, diffusion experiments), combined with geochemical modelling (e.g. Gaucher et al., 2009; Lerouge et al., 2020; Pearson et al., 2011).

Techniques allowing for a direct sampling of the free porewater in low-permeability rocks are limited, demanding and prone to experimental artefacts, such as oxidation and degassing. Besides long-term in-situ sampling in rock laboratories (Pearson et al., 2003; Vinsot et al., 2008a), high-pressure squeezing (Fernández et al., 2014; Mazurek et al., 2015; Wersin et al., 2016) and advective displacement techniques (Grambow et al., 2014; Mäder, 2018; Mäder and Waber, 2017b) have been developed. These methods mobilise a portion of the total porewater and it is assumed that this water provides a good approximation of the composition of the free porewater. In porewater squeezing large uniaxial stresses are applied to a rock sample confined in a squeezing cell to compress the rock skeleton and to displace a fraction of the porewater outwards into syringes. The technique of advective displacement applies a large hydraulic gradient to a confined drillcore sample, using an artificial porewater to displace the in-situ porewater to a sampling system. Extending the duration of advective displacement and using tracers also permits the quantification of multi component transport properties. The squeezing technique has already produced a substantial dataset of porewaters from bentonites (Fernández and Villar, 2010; Muurinen and Carlsson, 2007), from weakly consolidated clay rocks (De Craen et al., 2004a; Falck et al., 1990), and from clay rocks with a higher degree of consolidation and reduced water contents as low as 3 wt% (Fernández et al., 2014; Mazurek et al., 2015). In contrast, few experiments were performed with the advective displacement method (Grambow et al., 2014; Huclier-Markai et al., 2010; Mäder and Waber, 2017a; Mäder et al., 2004). Mäder (2018) reported two long-term advective displacement experiments, providing a detailed method description and insights into anion-specific transport properties and process understanding.

Between 2019 and 2022, Nagra, the Swiss National Cooperative for the Disposal of Radioactive Waste, performed a deep drilling campaign targeting the Opalinus Clay along the northern margin of the Swiss Molasse Basin as the potential host rock (Mazurek et al., 2023). In this context, the squeezing and advective displacement techniques were applied to rock samples from the Jurassic and Triassic profile sections of eight boreholes in three study areas. A unique dataset pertinent to the chemical composition of the porewater was obtained (59 squeezing and 33 advective-displacement tests). It illustrates the spatial distribution of porewater compositions and provides anchor points for the understanding of natural tracer profiles and the hydrogeological evolution of the system (Wersin et al., 2023). A comparison of porewater aliquots obtained by these two sampling procedures in combination with geochemical modelling identifies method-related challenges and provides insights into the representativeness of the sampled porewater aliquots for laboratory and in-situ conditions. The combined assessment of the natural variability and method related uncertainties forms the basis for the overall evaluation of porewater composition relevant for radionuclide solubilities, speciation and retention in performance assessment calculations, the stability of the barrier system and the dynamics of the geological system.

2. Geological setting

A detailed description of the geological setting and on the geochemical investigation program is provided by Mazurek et al. (2023). Briefly, nine deep boreholes penetrating the Mesozoic sedimentary sequence of central northern Switzerland were drilled in three study areas and provided more than 6 km of drillcore material (Fig. 1). The most western area Jura Ost (JO), with the boreholes Bözberg-1-1 (BOZ1-1) and Bözberg-2-1 (BOZ2-1), the central area of Nördlich Lägern (NL) with the boreholes Bülach-1-1 (BUL1-1), Stadel-2-1 (STA2-1), Stadel-3-1 (STA3-1) and Bachs-1-1 (BAC1-1) and the most eastern area Zürich Nordost (ZNO), with the boreholes of Marthalen-1-1 (MAR1-1), Trüllikon-1-1 (TRU1-1) and Rheinau-1-1 (RHE1-1). With the exception of Rheinau-1-1, substantial geological and geochemical datasets were obtained for each borehole.

The investigation program for porewater composition by the AD and SQ methods focused on the Opalinus Clay and its confining units, the latter including the underlying Lias (Staffelegg Fm.) and formations of the Dogger above the Opalinus Clay (denoted as D.A.O. in the following). The 100–120 m thick Opalinus Clay is the most clay-rich unit (clay minerals: 57 ± 10 wt%) and is laterally continuous with only minor facies changes, and was therefore displaying similar characteristics in all boreholes. The center of the Opalinus Clay is located at a depth of 500–600 m in study area JO, 850–950 in NL and 600–900 m in ZNO. The underlying Lias has a rather uniform thickness of 35–44 m but shows a large vertical heterogeneity with interstratified claystone-marl-limestone-sandstone units. The D.A.O. is heterogeneous in both the vertical and horizontal dimensions, encompassing mainly claystones, marls and limestones, with less frequent sandy lithologies. The clay minerals of the Opalinus Clay and its confining units include illite, predominantly illite-rich illite/smectite mixed layers, kaolinite, chlorite and chlorite-rich chlorite/smectite mixed layers. Detailed mineralogical and lithostratigraphic profiles are documented in Mazurek et al. (2023).

3. Methods

3.1. Sampling and sample preservation

In total 59 and 33 drillcore samples were processed for SQ and AD experiments, respectively. These were distributed across the clay rich units of 8 boreholes in the 3 study areas, whereof 51 (SQ) and 30 (AD) originated from the Opalinus Clay and the confining units and are discussed here. In the sample selection procedure, preference was given to rather homogenous, unfractured drillcore samples displaying few local heterogeneities, such as larger pyrite or siderite lenses, or macro-fossil accumulations. These heterogeneities were detected on-site by photoscanning and in case of AD samples supplemented by X-ray computed tomography (CT) scans. Note that for both the SQ and AD techniques, mainly clay-rich lithologies (>30 wt% clay minerals) were sampled from all geological units because of their higher porosity and therefore a better chance of successful porewater extraction. The drillcore samples of 9.5 cm in diameter and ~20 cm length were cleaned on-site from drilling fluid and preserved from oxidation and evaporation by layers of vacuum-sealed polyamide/polyethylene and plasticized aluminium bags within approximately 20 min after core retrieval. Samples were stored at 4 °C until preparation for AD and SQ experiments. Tests using

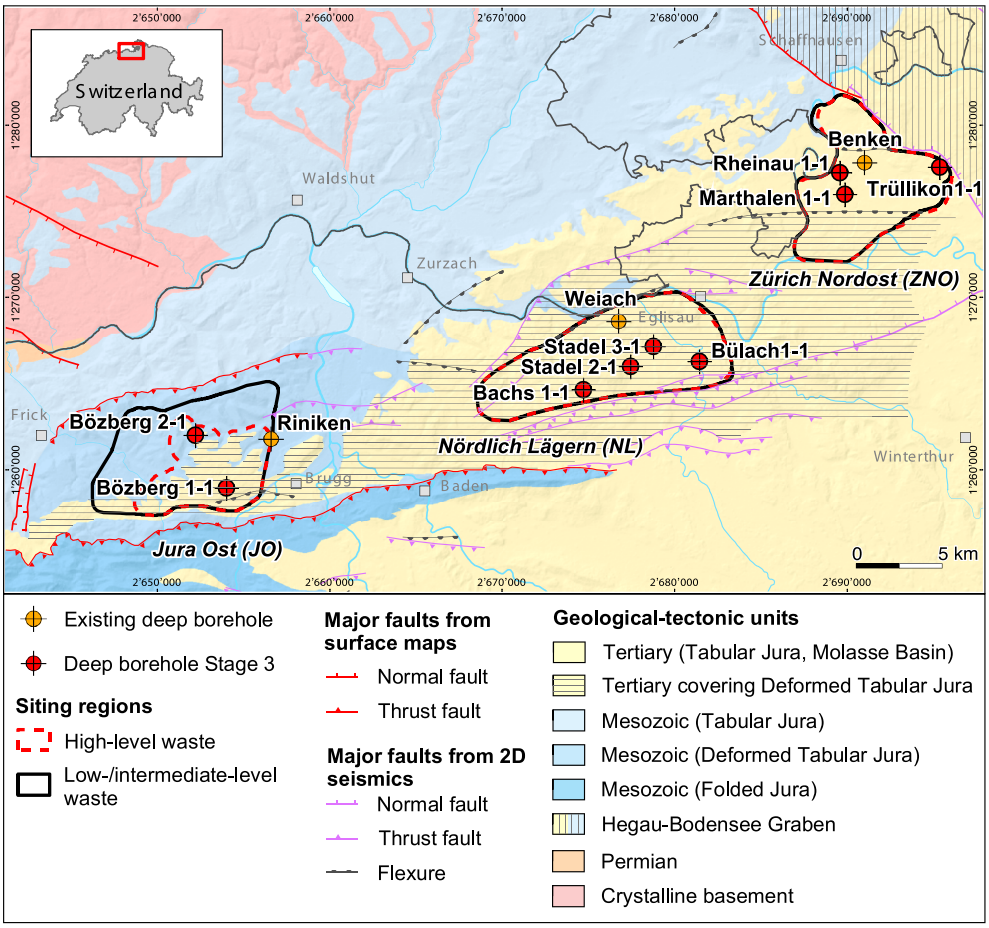

Fig. 1. Geological-tectonic map with locations of study areas and boreholes (adapted from Madritsch (2015)).

preserved samples from older boreholes indicated that the multiple sample wrapping and subsequent cold storage successfully prevented oxidation and evaporation, based on the fact that SO_4 contents and water-isotope compositions measured on these samples were near-identical to those obtained from adjacent samples analysed shortly after drilling several years before. Storage time for AD samples was, with few exceptions 1–6 weeks. SQ samples were shipped to CRIEPI, Japan, for high pressure squeezing, which increased the time between drilling

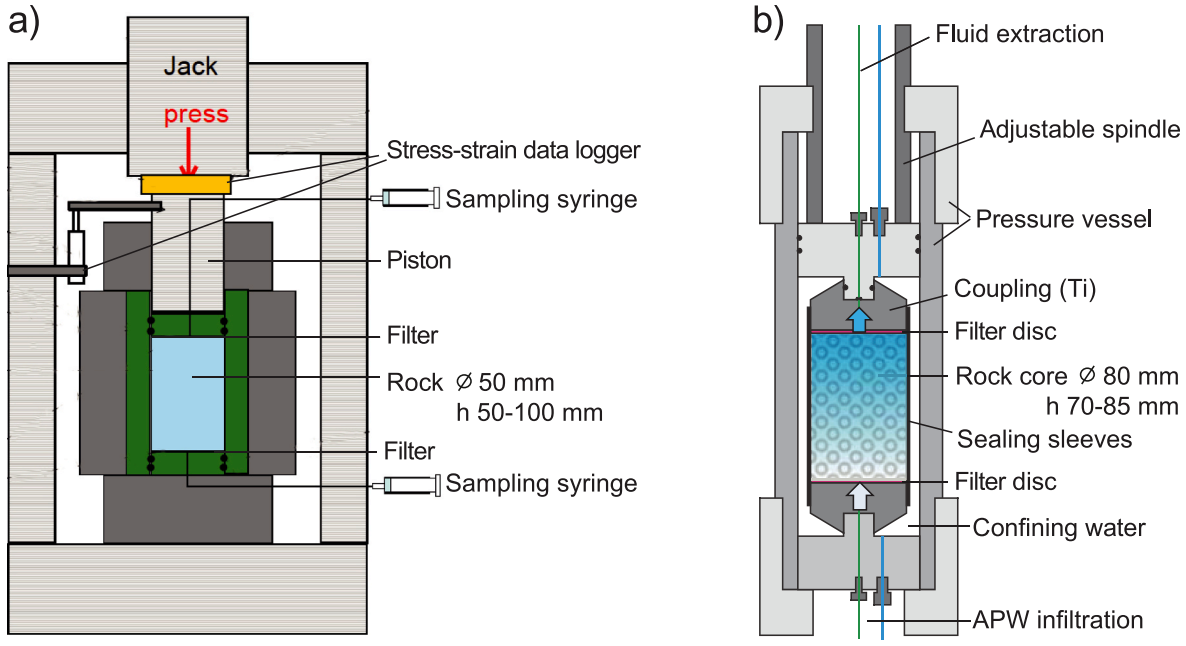

Fig. 2. Schematic of the squeezing (a) and advective displacement (b) apparatus. Re-drawn from Mazurek et al. (2015) and Mäder (2018).

and sample preparation to 3 weeks to a few months. The cooling chain was maintained during transport and storage.

3.2. Squeezing experiments (SQ)

In the squeezing technique, a piston applies pressure perpendicular to the bedding in order to retrieve porewater from the saturated rock samples. The squeezing tests of the present study were performed at the Central Research Institute of Electric Power Industry (CRIEPI), Japan, following the procedure detailed in Mazurek et al. (2015) and sketched in Fig. 2a. Briefly, a multi-facet prismatic rock sample obtained by dry cutting of the drillcore sample was inserted into the squeezing chamber of 5 cm diameter and 10 cm height. Fiberglass filters (Whatman GF/B 1.0 μm, 47 mm diameter) were attached to the upper and lower sample surfaces. Within about 10 min after the onset of the initial squeezing pressure most of the gas phase from the dead-volume was expelled and water filled the capillary tubes leading to the sampling syringes on both ends of the chamber. At this point, the air was removed from the syringes and the first water aliquot was sampled. First water aliquots were typically obtained at 200 MPa (38 out of 59 samples), while for some samples higher pressures of 300 MPa (13 samples), 400 MPa (3 samples) and 500 MPa (5 samples) were required. These latter samples were characterized by a low water content of <4 wt%, typical for samples with a lower clay content (see Mazurek et al. (2023) for the correlation of clay and water contents). Collection of the first water sample was finalized after 2–8 days if obtained at 200 MPa but extended up to 19 days for samples that required higher pressures before yielding water. The sample mass obtained at the first successful pressure amounted to 0.13–2.9 g, corresponding to 1–12% of the total porewater of the rock samples. One to three additional porewater samples were obtained by increasing the pressure in intervals of 100 MPa with a standing time of 2–3 days at each step, resulting in a total squeezing time of around 10–20 days per sample. Porewaters sampled at each pressure step in the top and bottom syringe were combined in glass bottles, stored at 4 °C and then sent to University of Bern, for chemical analysis.

3.3. Advective displacement experiments (AD)

Advective displacement (AD) experiments were performed at the University of Bern, applying the set-up described in detail by Mäder (2018) and RWI (2020) and depicted in Fig. 2b. The principle relies on the advective displacement of the sample porewater by an artificial porewater (APW) applying a large hydraulic gradient to a confined rock sample while keeping the rock texture intact. The APW was spiked with a water tracer (^2H), was free of Br^-, and exhibited a similar but still distinct composition as the expected sample porewater in order to trace the breakthrough of the APW and to characterize water and solute transport (Tables SI–1). A central cylindrical drillcore segment of approximately 8 cm in length and diameter was obtained by dry cutting and subsequent machining on a lathe to remove the potentially contaminated outermost layer. The AD sample cores were sandwiched between two filter discs and titanium adapters and wrapped in Teflon tape and a double layer of latex-sleeves (Model 28-WF4075, Wykeham-Farrance) to separate the core from the confining fluid (1:1 mix of tap and deionised water). A confining pressure of around 6 MPa was maintained throughout the experiments by pressurizing a supply tank with Ar that remained connected to the pressure container via steel tubing. This set-up was - after several experiments - suspected to allow gas, vapour and potentially microorganisms to migrate from the confining fluid into the core. Thus, later samples were additionally wrapped by elastic electric tape and a rather sturdy cold-shrinking tube (3 M Kaltschrumpfschlauch 8430.9, EPDM, 93.7/42.6/229). The APW was injected via a PEEK-capillary through the Ti-headpiece from the bottom applying infiltration pressures of a 4.5–5.0 MPa by pressurizing the APW tank with He. Depending on the sample length, hydraulic gradients of 5′000–7′000 m_{H2O}/m (50–70 MPa/m) were applied. The exfiltrating fluid was passed via PEEK capillaries through an electric conductivity cell (Metrohm) before it was collected in the sampling syringes (polypropylene syringes with rubber seals, ethanol washed). The time from starting the infiltration at the bottom and collection of the first sample at the top strongly depended on core permeability and varied between 1 and 20 days (approx. 1 week for the Opalinus Clay). The early exfiltrating porewater was sampled and analysed in aliquots of 0.5–3 g. A small initial aliquot (~0.3–0.5 g) was discarded because the composition of the porewater close to the surface of the core sample might be affected by evaporation during sample preparation or by very near-surface oxidation. The early porewater samples (1 discarded and 2 analysed) were in most experiments obtained in 9–40 days of displacement and corresponded, including the discarded volume, to 3–16 % of the total porewater in the core sample. A detailed listing of the experimental set-up (wrappings, filters), conditions (confining and infiltration pressures) and sample characteristics (time until first fluid drop) is provided for each experiment in the Supporting Information (Tables SI–2).

3.4. Analyses of squeezed and displaced porewater aliquots and rock samples

Major ion analyses of SQ and AD aliquots were performed at the University of Bern, Switzerland, following the procedures detailed in RWI (2020). AD aliquots were diluted gravimetrically shortly after sampling of a syringe, whereas SQ aliquots were sealed and shipped from CRIEPI (Japan) to Bern, before dilution and analysis. Given the filtration in the squeezing and advective displacement devices, no additional filtration step prior to sample dilution was performed.

Cations (Na, K, NH_4, Ca, Mg, Sr) and anions (F, Cl, Br, NO_3, SO_4) were analysed by a Metrohm 850 Professional IC. This was done for cations with a Metrohm Metrosep C4-150/4.0 separation column (Nr. 6.1050.420) and an eluent of 1.7 mM HNO_3– and 0.7 mM dipicolinic acid and for anions with a Metrosep ASupp7-250/4.0 column (Nr. 6.1006.630) and a 3.6 mM Na_2CO_3 eluent. For selected ions (Sr, Ba, Fe, Si) the ICP-OES technique was applied, using an axial ICP-OES Varian 720 ES. Total dissolved inorganic carbon (TIC) and dissolved organic carbon (TOC) were measured by infrared spectrometric techniques (Analytic Jena Multi N/C 2100 S with NDIR-detector). TIC was measured directly after oxidation of the dissolved inorganic C to CO_2 using 10% phosphoric acid (p.a., Merck) and TOC was determined as the difference to the total carbon (TC) as determined by thermocatalytic oxidation of the solution at 750 °C and oxidation of all carbon using a platinum catalyser and oxygen. The δ^2H values were analysed using a Picarro L2120-i cavity ring down spectrometer (CRDS) with vaporisation module V1102–I as described by Aschwanden et al. (2023a). To account for small sample volumes, micro-sample inserts of 100 μL were used.

The pH of AD samples was measured in-line, by temporally diverting the normal sampling path to an in-line pH flow-through cell and on a small sample aliquot (50–100 μl) directly after sampling a syringe. Both measurements were done with an Orion ™ Ross glass combination micro pH-electrode 8220BNWP with either an Orion Versastar pH-meter (laboratory) or a JUMO Ecottrans pH transmitter (in-line) connected to a data acquisition system. The same electrode was applied for the pH measurement of SQ aliquots, however, after longer sample storage due to the transport from Japan to Switzerland.

Water content (gravimetric water loss at 105 °C) was determined on sample discs cut adjacent to the SQ and AD sample. Bulk and clay mineralogy (powder X-ray diffraction) were quantified for adjacent (AD) or post-experimental (SQ) material. Exchangeable cations and cation exchange capacity (Ni-en method, Solid/liquid ration ~1:1, anaerobic conditions) were measured for samples adjacent to AD experiments, only. The entire sample workflow and all methods are described in detail in RWI (2020).

4. Results and discussion

4.1. Evolution of porewater composition in SQ and AD experiments

For the SQ experiments, the major-ion composition of waters squeezed at the lowest pressure step is provided in Tables SI–3, whereas those at higher pressure steps can be found in the respective data report (see Supporting Information for a list of references). The porewater chemistry of water samples obtained at increasing pressure steps show a characteristic evolution, as already observed and discussed in detail by Mazurek et al. (2015) for a set of comparative squeezing experiments from the Opalinus Clay and confining units of the deep borehole of Schlattingen, Northern Switzerland. Ionic strength, dominated by Na^+ and Cl^- in this study, decreases with sequential squeezing at increasing pressure. At each squeezing step, the expelled porewater is however more saline compared to the bulk porewater remaining in the clay, as evidenced by tracking the chloride mass balance. Generally, the concentrations of the monovalent ions (Cl^-, Br^-, Na^+ and K^+) decrease, which was previously attributed to ion filtration, whereas those of Ca^{2+}, Mg^{2+} and SO_4^{2-} tend to remain constant or even increase, due to the increasing mineral solubilities at higher pressure (Mazurek et al., 2015). The first water aliquot is considered to be close to the free porewater composition of the sample (for discussion see Mazurek et al. (2015)).

For the AD experiments, the composition of the first 2 analysed aliquots is provided in the Supporting Information (Tables SI–4). It is expected that the early aliquots show a constant chemical composition, as they are not yet affected by the advective or diffusive breakthrough of the injected APW (Mäder, 2018). However, this is not the case for all samples and in several experiments from NL and ZNO an apparent immediate evolution towards the less saline APW was observed. The exact reason for this is not resolved at the present stage and could be related to some disturbances at the surface of the sample. A rapid admixing of the infiltrating APW via diffusion or advective flow in preferential pathways cannot be excluded either, although the evolution of the water tracer added to the APW (^2H: 100‰ VSMOW) gave no indication for a significant APW contribution. The difference between the first and second analysed aliquot however remained within 10% for most samples and major ions, without any clear dependency on sampling time. Therefore, the average of the two first sampled aliquots was considered as the best approximation of the free porewater.

4.2. Porewater composition of AD and SQ samples

4.2.1. Regional characteristics

The lateral and vertical distribution of the free porewater composition in argillaceous rock sequences such as the Opalinus Clay and its confining units inherits a signature of the past hydrogeochemical evolution. Its interpretation requires representative and well-constrained porewater compositions, which reproduce the natural variability beyond experimental uncertainty. Fig. 3 displays the major ion concentrations in the porewater samples from the Opalinus Clay and the confining units, obtained by SQ (lowest pressure step) and by AD (average of the two early aliquots). The porewater compositions derived by both methods consistently reflect the characteristics of the three study areas and geological units. Porewaters in NL and ZNO are of a Na–Cl type with a similar salinity, whereas the porewaters of JO are more dilute and of a Na–Cl-(SO_4) type according to the classification scheme of Jäckli (1970). Table 1 provides the composition of selected Opalinus Clay porewaters in the 8 boreholes as determined with AD and SQ on rock samples of comparable depth and sample characteristics. Between the three study areas, Cl concentrations in the free porewater of Opalinus Clay vary by a factor of 4–7, reflecting local hydrogeochemical controls such as the proximity of the aquifer infiltration zone in the comparable shallower JO region or the remaining impact of deep salt dissolution in the SE of NL (Wersin et al., 2023).

The geochemical depth profiles of Cl obtained by each of the two methods (Fig. 4a) display similar trends, characterized by rather constant values across the Opalinus Clay and a salinity decrease within the confining units. The most prominent salinity decrease is observed in the Lias of the ZNO and slightly less in JO, reflecting the exchange with a low salinity aquifer in the Keuper around 15–20 m below the base of the Lias (Mazurek et al., 2023; Wersin et al., 2023). The diffusive exchange with the aquifer is also manifested in the pronounced increase in the SO_4/Cl ratios with depth in the Lias of ZNO and JO, while in NL this ratio remains close to the ratio of seawater (Fig. 4b). In JO, significantly higher SO_4/Cl ratios than in NL and ZNO are observed across the entire profile, which reflects the diffusive exchange with diluted groundwaters in equilibrium with sulphate mineral phases. A detailed discussion of Cl

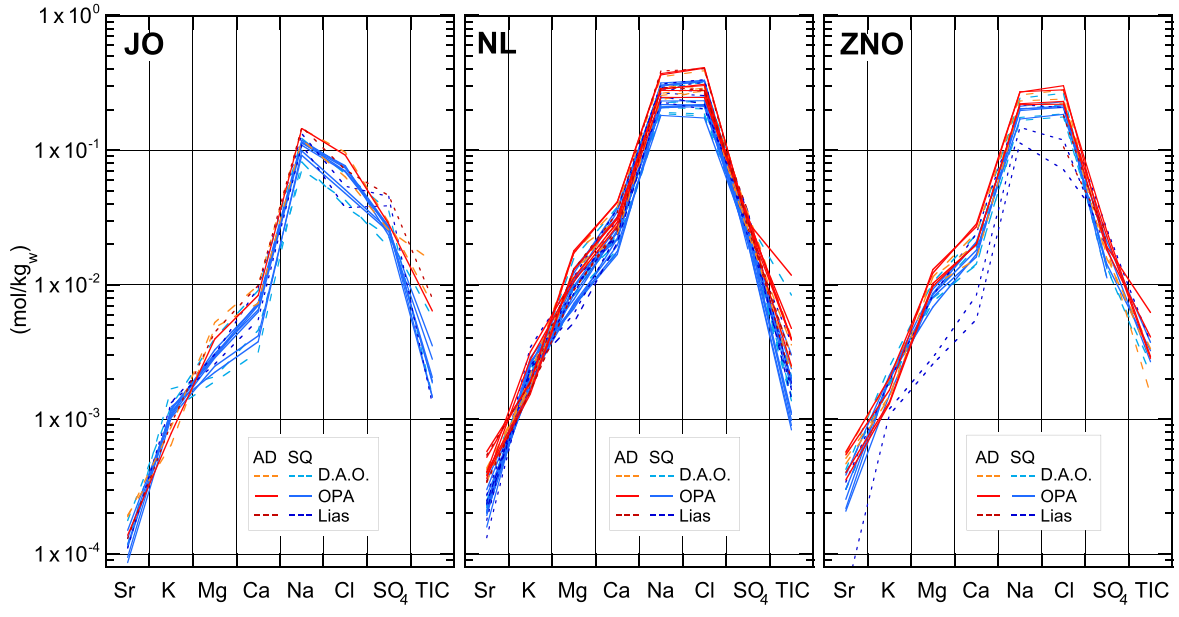

Fig. 3. Schoeller plots of porewater compositions obtained by the SQ (blue) and AD (red) methods for the Opalinus Clay, Dogger above Opalinus Clay (D.A.O.) and Lias in the three study areas Jura Ost (JO), Nördlich Lägern (NL) and Zürich Nordost (ZNO).

Table 1
Composition of selected Opalinus Clay porewater samples as determined by AD and SQ. TIC refers to the values corrected for loss of CO_2 to calcite equilibrium (4.3.3); kg_w: kg of water, n.d.: not determined.

		JO				NL						ZNO			
		BOZ2-1	BOZ1-1		BAC1-1	STA2-1		STA3-1		BUL1-1		MAR1-1		TRU1-1	
		SQ	AD	SQ	AD	SQ	AD	SQ	AD	SQ	AD	SQ	AD	SQ	AD	SQ
mean depth	(m)	545.41	575.26	554.36	910.21	896.5	900.81	850.29	849.98	859.37	987.55	990.66	702.4	698.47	926.14	904.86
pH_{Lab}		8.85	7.37	8.99	7.46	8.60	7.54	8.33	7.67	8.28	7.38	8.10	7.67	8.40	7.27	n.d.
$pH_{calcite\ eq.\ 25°C}$		7.50	6.95	7.43	6.62	7.11	6.65	7.03	6.66	7.12	6.04	6.61	6.89	6.77	6.98	n.d.
Na	(mol/kg_w)	9.15E-2	1.45E-1	1.14E-1	2.83E-1	2.09E-1	2.47E-1	1.81E-1	2.77E-1	2.18E-1	3.70E-1	2.98E-1	2.18E-1	1.70E-1	2.71E-1	2.02E-1
K	(mol/kg_w)	1.03E-3	7.88E-4	1.08E-3	1.54E-3	1.87E-3	2.79E-3	1.94E-3	3.16E-3	2.62E-3	1.87E-3	1.87E-3	1.31E-3	1.51E-3	2.03E-3	1.94E-3
Mg	(mol/kg_w)	2.48E-3	3.94E-3	3.28E-3	1.30E-2	9.76E-3	1.06E-2	7.27E-3	1.13E-2	6.96E-3	1.72E-2	1.22E-2	9.74E-3	8.49E-3	1.22E-2	8.62E-3
Ca	(mol/kg_w)	4.17E-3	8.34E-3	7.14E-3	3.16E-2	2.68E-2	2.74E-2	1.96E-2	2.91E-2	1.68E-2	4.13E-2	3.68E-2	2.00E-2	1.80E-2	2.83E-2	2.08E-2
Sr	(mol/kg_w)	8.62E-5	1.38E-4	1.50E-4	3.84E-4	2.06E-4	3.63E-4	2.00E-4	4.05E-4	1.93E-4	5.75E-4	3.48E-4	3.55E-4	2.08E-4	5.72E-4	3.02E-4
Cl	(mol/kg_w)	4.76E-2	9.19E-2	6.99E-2	3.08E-1	2.18E-1	2.46E-1	1.73E-1	2.76E-1	2.15E-1	4.11E-1	3.26E-1	2.19E-1	1.84E-1	2.80E-1	2.13E-1
Br	(mol/kg_w)	5.26E-5	1.09E-4	7.23E-5	3.54E-4	2.74E-4	2.60E-4	2.11E-4	3.04E-4	2.69E-4	2.48E-4	2.21E-4	9.91E-5	7.87E-5	8.46E-5	7.97E-5
SO_4	(mol/kg_w)	2.48E-2	2.82E-2	2.69E-2	2.87E-2	2.46E-2	3.21E-2	2.26E-2	3.23E-2	2.55E-2	2.92E-2	2.37E-2	2.27E-2	2.09E-2	2.48E-2	1.34E-2
TIC	(mol/kg_w)	2.80E-3	7.14E-3	2.42E-3	5.18E-3	1.50E-3	3.99E-3	2.02E-3	5.13E-3	2.41E-3	2.56E-2	4.37E-3	3.39E-3	5.28E-3	3.20E-3	n.d.
Ionic strength	(mol/kg_w)	1.19E-1	1.84E-1	1.48E-1	3.99E-1	3.02E-1	3.43E-1	2.49E-1	3.77E-1	2.87E-1	5.16E-1	4.20E-1	2.96E-1	2.48E-1	3.71E-1	2.77E-1
charge balance	(eq/kg_w)	5.38E-3	5.97E-3	1.00E-2	3.55E-3	1.57E-2	1.10E-2	1.60E-2	1.59E-2	8.69E-4	8.85E-3	2.17E-2	1.07E-2	−5.43E-3	2.18E-2	2.06E-2
error	(%)	2.82	1.93	4.15	0.51	3.04	1.86	3.73	2.42	0.17	0.97	2.96	2.08	−1.27	3.36	4.23

depth profiles and the exchange of porewaters with the surrounding aquifers, illustrating the context of the AD and SQ data, is provided in Wersin et al. (2023).

Similar trends as for Cl are reflected in the Ca profiles, but the scatter is generally somewhat larger (Fig. 4c). While the major regional difference between the profiles from JO and NL/ZNO are well-resolved independent of the sampling method, a distinct and systematic offset in the solute concentrations between aliquots obtained by AD and SQ experiments overprint the smaller regional variability in the ZNO/NL study areas. In each borehole, the discrepancy exceeds the concentration range encompassed by the small depth gradients within the Opalinus Clay described by either method. This precludes small-scale natural heterogeneity of the free porewater composition as an explanation for the observed differences and indicates inherent differences in the porewaters obtained by AD and SQ.

4.2.2. *Method comparison*

The porewater compositions obtained by SQ and AD experiments in the Opalinus Clay can be directly compared, given the quite limited variability with depth in each borehole. Deciphering and quantifying communalities and systematic differences set the basis for an improved understanding of the sampled porewaters with respect to potential method-related artefacts and sampling characteristics.

A consistent picture emerges with porewaters from AD experiments exhibiting ion concentrations 10–40% higher than respective porewaters obtained by SQ (Fig. 5a). In 5 out of 7 borehole datasets, the offset in Cl concentrations is even more closely constrained to 25–30%. Note that the tendency of higher salinity in AD samples versus SQ samples is also observed for the adjacent confining units, although less evident and consistent due to a generally larger heterogeneity and the presence of large vertical concentration gradients particularly in the Lias (Mäder and Wersin, 2023; Wersin et al., 2023). In an earlier study focused on the Schlattingen borehole, a similar offset for an AD and SQ sample from the Opalinus Clay was determined, whereas for two samples from the D.A.O. no systematic picture was obtained (Wersin et al., 2020).

Despite the offset in the absolute concentrations obtained by both methods, there is a general high consistency in the ion ratios (Fig. 5b). The apparent discrepancy in the SO_4/Cl ratio in BOZ1-1 and TRU1-1 has to be interpreted with care, given the distinct vertical gradient of SO_4 concentrations and SO_4/Cl ratios with depth and the small number of analyses (Fig. 4). Br/Cl ratios are almost identical in porewater samples obtained by both methods and well in line with the large data set obtained by aqueous extraction (Wersin et al., 2023). Both anions are assumed to be non-reactive and of high relevance for the understanding of the provenance and evolution of the porewaters over geological timescales.

A tendency towards higher Mg/Na and Sr/Na ratios in aliquots from AD experiments compared to SQ aliquots from the same borehole is observed. The contrary is the case for the K/Na ratio, with significantly higher values obtained by SQ experiments. Fernández et al. (2014) also observed relatively high K concentrations in squeezed samples of Mont Terri compared to borehole waters and attributed this to a temperature effect on the K selectivity coefficients. Given the comparable temperatures prevailing in the AD and SQ experiments, this explanation is considered inappropriate at least in the context of the present study.

4.2.3. *Implications for the porosity domains sampled by AD and SQ experiments*

In the light of the two distinct mechanisms applied for the mobilization of the free porewater from the rock samples, a large hydraulic gradient in AD experiments versus the mechanical compaction involving shear movements and deformation of the pore space in SQ experiments, differences in the composition of the sampled porewater can be expected. In the following, we will evaluate how the observed higher salinity in AD versus SQ aliquots and the shift in some cation ratios, in

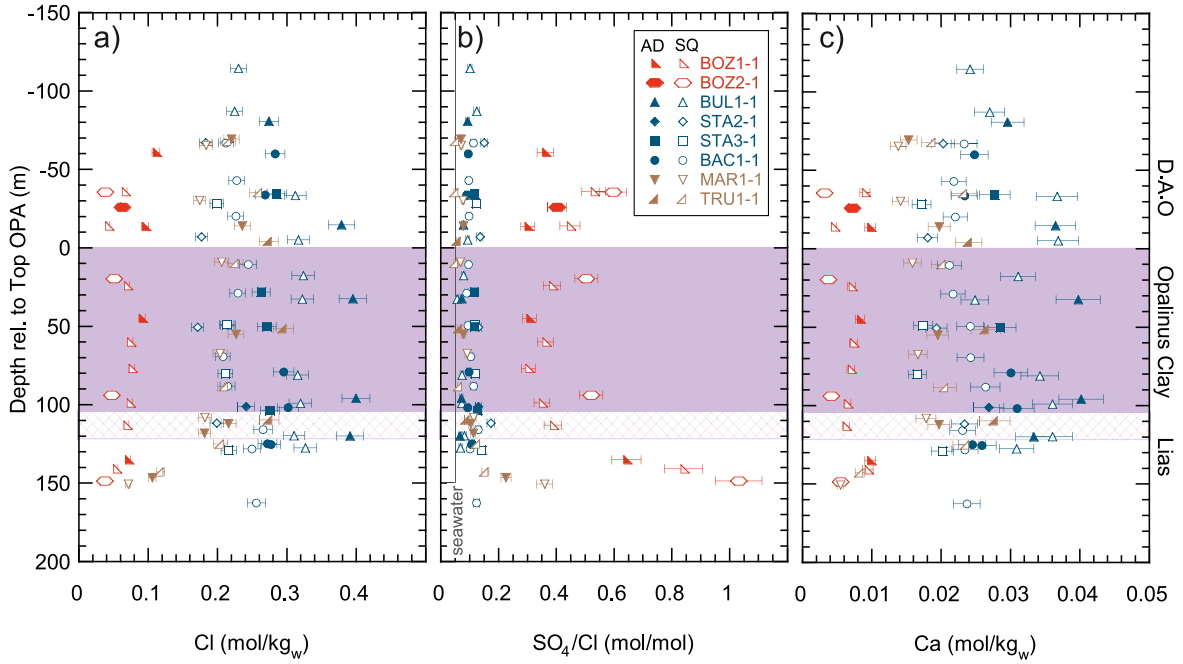

Fig. 4. Profiles of Cl concentrations (a), SO_4/Cl molar ratios (b) and Ca concentration (c) as obtained by AD (filled symbols) and SQ (open symbols). Depth is given relative to the top of the Opalinus Clay (top OPA core depth (m): BOZ1-1:530.28; BOZ2-1: 451.54; BUL1-1: 891.70; STA2-1: 799.67; STA3-1: 779.26; BAC1-1: 808.34; MAR1-1: 590.35; TRU1-1:816.42). Hashed area indicates the variable thickness of the Opalinus Clay intersected in the boreholes. Colours distinguish the three study areas Jura Ost (red), Nördlich Lägern (blue) and Zürich Nordost (brown).

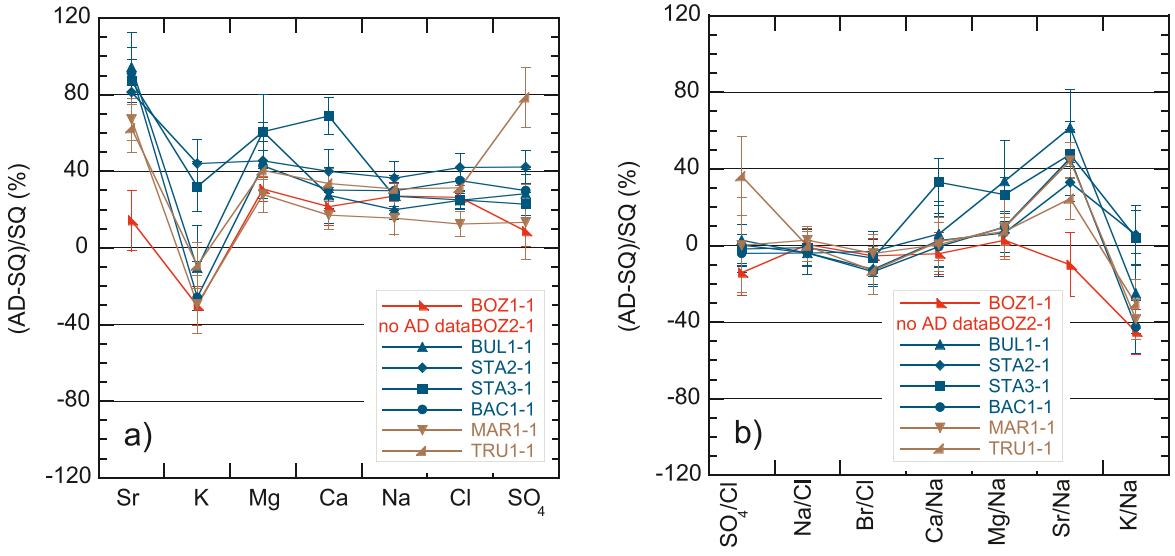

Fig. 5. Difference of average concentrations (left) and molar ratios (right) in AD vs SQ experiments in Opalinus Clay porewater for each borehole in the three areas JO (red), NL (blue) and ZNO brown). Error bars represent the propagated uncertainty of either the analytical uncertainty or the standard deviation over the Opalinus Clay samples. These were evaluated for each method and borehole separately. Whichever was larger for each method was included in the error-propagation.

particular in K/Na may relate to method specific artefacts and/or mobilization of different porewater domains.

Experimental uncertainties in AD experiments involve potential evaporation at the sample surface during the preparation, an early breakthrough of the artificial porewater or the intrusion of the confining water. While the first process could explain an increased salinity in AD versus SQ aliquots, it does not easily explain the observed differences in some cation ratios. The admixture of APW or confining water would have reduced the salinity in the AD aliquots for samples from NL and ZNO, thus indicating even higher concentrations in the free porewater. Because the APW contained the water tracer (^{2}H), such an artefact related to early APW breakthrough can be excluded.

The major processes commonly discussed in the context of SQ experiments are ion filtration effects and pressure induced mineral dissolution (Fernández et al., 2014; Mazurek et al., 2015). The latter process may be disregarded in the present context, as it would rather increase the salinity. Ion filtration effects may become significant beyond a threshold squeezing pressure, which is assumed to be specific to each rock (lithology, degree of compaction (Fernández et al., 2014)). It may thus be suspected that in the present study the threshold squeezing

pressure has already been exceeded by the lowest pressure step. For the cations, the strongest effect would be expected for K, given its large ionic radius, and in consistency with experimental data pertinent to geological membranes (Hanshaw and Coplen, 1973; Iyer, 1990; Kharaka and Berry, 1973; Kharaka and Smalley, 1976). Indeed, K shows the strongest decrease with squeezing pressure (4.1). However, the very characteristic higher values for K in SQ aliquots compared to AD experiments, speaks against this argument and renders ion filtration a less likely explanation.

Hence, the differences may rather relate to differences in the kinematic porosities sampled by the two methods, which are not necessarily identical to the geochemically free porosity. Fig. 6 sketches the distribution of anions and cations with increasing distance from the clay surface. The negative charge at the mineral surface is counterbalanced by sorbed cations in the Stern layer and by a surplus of cations in the diffuse layer (Tournassat et al., 2009). While anions are completely excluded from the Stern layer, their concentration increases exponentially with distance from the surface (diffuse layer) according to theories based on the Poisson-Boltzmann equations. In principle, the ratio of divalent/monovalent cations increases towards the negatively charged surface (Hedström and Karnland, 2011), whereas no major shift in the ratio of cations of the same valence would be expected. In the case of the Opalinus Clay and clay rich confining units however, the dominating clay minerals are illite-rich illite/smectite mixed layers (Mazurek et al., 2023), which exhibit sites with a high selectivity for K (Meunier and Velde, 2004), thus increasing K at the mineral surface. The thickness of the diffuse layer depends on various factors such as the charge density of the surface, the charge of the anion and the ionic strength of the porewater, with the latter being proportional to the Debye length, which itself is proportional to $1/\sqrt{ionic\ strength}$ of the free water (Tournassat and Appelo, 2011). In small pores associated with clay aggregates, opposing diffuse layers may overlap and exhibit interlayer (IL) like properties, i.e. being largely devoid of anions. Zwahlen et al. (2023) estimated for the clay rich rocks of the Opalinus Clay and confining units that IL and IL like pores ($r < 2$ nm) may account for about half of the anion depleted porosity domain. In turn, the other half may be associated with larger pores in which the fraction of the volume affected by the anion exclusion effects declines with increasing pore size and with increasing salinity.

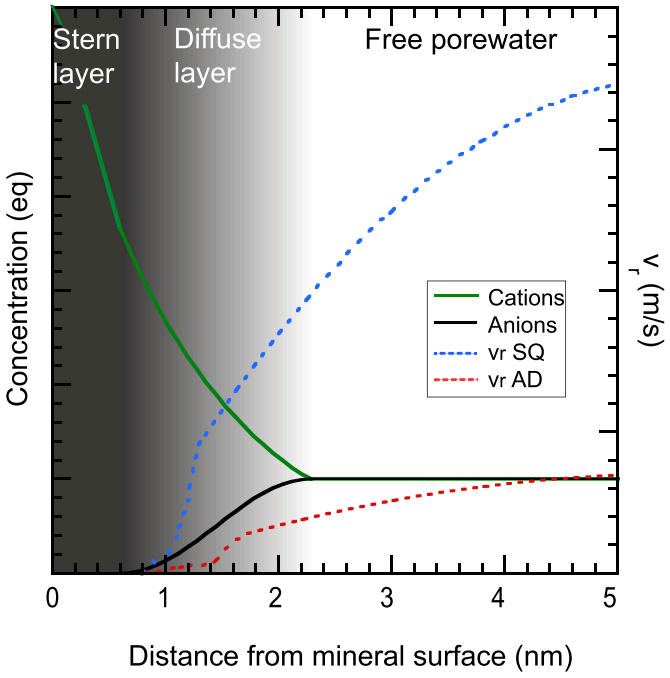

Fig. 6. Sketch visualizing the concentration gradients of anions (black) and cations (green) with increasing distance from a charged clay surface. Dotted lines depict flow velocity distributions (v_r) considering a higher average flow in SQ than in AD (see text for more information).

While the distribution of anions and cations over the porosity domain is an intrinsic characteristic of the rock sample, the kinematic porosity depends on the extraction procedure. Both, AD and SQ experiments involve a pressure driven Poiseuille flow. Due to the interaction of water molecules with the clay mineral surfaces two velocity fields evolve, a reduced velocity field in the interfacial region and a velocity distribution in the bulk water (Sun et al., 2019). Fig. 6 qualitatively depicts the flow velocity distributions in SQ and AD experiments, taking into account that the overall flow is higher in SQ than in AD experiments. It can be envisioned that the higher velocity in SQ increases the kinematic porosity as it shears more easily water closer to the clay surfaces. In addition, SQ is associated with a reduction in the total pore volume and given squeezing pressures above the swelling pressure of interlayer pores, a decrease of interlayers and expulsion of almost solute free water might contribute as well. In theory, interlayer distance is adapted to the lithostatic pressure and decreases when a higher experimental confining pressure is applied, which is already the case at the first squeezing pressure of 200 MPa. Furthermore, some of the IL like pores decrease instantaneously if the confining pressure is increased (Hsiao and Hedström, 2017). Both, the shearing-off of a larger fraction of the diffuse layer and the expulsion of water from interlayers and interlayer like pores, can explain diluted SQ aliquots without larger changes in the major ion ratios. While the contribution of the latter process is rather independent of the porewater salinity, the mobilization of diffuse layer water not only in SQ but also in AD may increase with decreasing salinity. A comparison of AD and SQ data with Cl concentrations obtained by upscaling aqueous extracts with diffusion data, as detailed in Zwahlen et al. (2023), indeed suggests a dilution effect in the case of the less saline JO samples for both AD and SQ but not for the more saline NL/ZNO porewaters. The compression of the diffuse layer during the squeezing process may furthermore alter the cation exchange equilibrium close to the surface and exchange some of the K from the Stern layer on the illite surface with divalent cations, thereby increasing the K concentration in the squeezed porewater aliquot.

4.3. *Representativeness of sampled porewaters for in-situ conditions*

In-situ porewaters in clay formations are on the one hand controlled by the local hydrogeochemical history constraining e.g. Cl concentrations (section 4.2.1) and on the other hand by internal controls, including i) the equilibrium with the rock forming minerals such as carbonates, silicates and sulphates, and ii) the cation population of the exchanger (clay minerals). The internal controls, in particular mineral equilibria, depend on temperature and pressure conditions. Porewater compositions may thus differ for laboratory (25 °C) and in-situ conditions, where temperatures at the level of the Opalinus Clay and its confining units range from 25 to 40 °C and 30–50 °C in JO and NL/ZNO, respectively. The consistency of experimentally derived porewater compositions with these internal controls may constrain the representativeness of the waters for laboratory and in-situ conditions.

To this end, mineral saturation indices (SI) for the porewater compositions derived by AD and SQ were calculated with the PHREEQC code (v.3.7.3) (Parkhurst and Appelo, 2013) using the Nagra/PSI database v. 12/7 (Thoenen et al., 2014) for a laboratory temperature of 25 °C. Additional calculations at in-situ temperature were performed with the Thermoddem database (Blanc et al., 2012). A full geochemical porewater model for the laboratory conditions was applied to compare the cation composition expected from cation exchanger data with the obtained porewaters (section 4.4).

4.3.1. *Mineral equilibria*

Fig. 7 (top) visualizes the saturation indices (SI) under laboratory conditions (25 °C) for the major controlling minerals of the samples from the Opalinus Clay and confining units. The most dominant feature is a

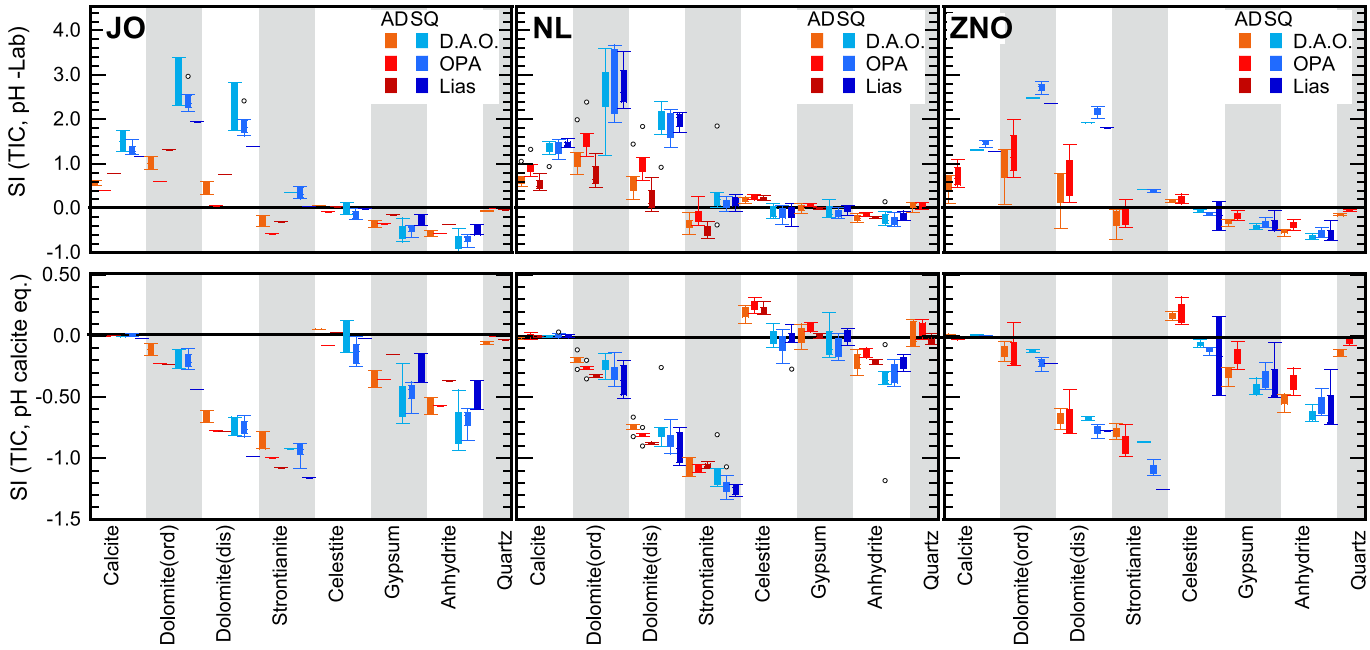

Fig. 7. Box-plots of mineral saturation indices (SI) for AD (red colour scheme) and SQ (blue colour scheme) samples from the Dogger above Opalinus Clay (D.A.O.), Opalinus Clay (OPA) and Lias in the three study areas Jura Ost (JO), Nördlich Lägern (NL) and Zürich Nordost (ZNO). Top panel is calculated with TIC and pH as measured in the laboratory (for 25 °C), whereas bottom panel indicates SI after correcting for outgassing of CO_2 until calcite equilibrium (see section 4.2 for further explanation). Note the different y-axis scales. In the case of the AD experiments, SI are based on a generic composition obtained by the averaging of the two early sample aliquots. It was however assured by individual calculations that the averaging did not induce a bias in the SI.

high oversaturation of all samples with regard to the carbonate minerals. For AD samples, $SI_{calcite}$ of 0.7 ± 0.3 and 0.5 ± 0.3 for the pH_{lab} and pH_{inline}, respectively were derived, whereas for SQ samples $SI_{calcite}$ ranges from 0.9 to 1.7. Given the generally fast attainment of the calcite equilibrium, this points to a disturbance of the pH/pCO_2 system in the samples induced by the extraction method and/or storage, which is addressed in detail in section 4.3.3. With an adjustment of the pH/pCO_2 system to calcite equilibrium (Fig. 7 bottom), the oversaturation of porewaters with regard to the dolomite varieties and to strontianite (SQ only) changes to undersaturation. In the case of dolomite undersaturation increases with depth in particular in the study areas NL and ZNO (see section 4.3.2). Under the assumption of calcite equilibrium and 25 °C, porewaters are closer to equilibrium with regard to the ordered dolomite variety of the Nagra/PSI database (see review of dolomite data in Hummel and Thoenen, 2022).

The SI of gypsum evidences a dissimilarity in porewaters between NL and the other two regions (Fig. 7). Porewaters of NL are close to gypsum equilibrium (SI -0.2 to +0.2) in particular in boreholes BUL1-1 and BAC1-1, whereas the porewaters of JO and ZNO show undersaturation that slightly decreases with depth. This is also manifested in the more pronounced increase of the SO_4/Cl ratio with depth in the latter two regions reflecting the diffusive exchange with the underlying Triassic aquifers (Fig. 4). All samples are undersaturated with regard to anhydrite considering the lab temperature of 25 °C. However, in some samples from the NL boreholes, in-situ temperatures above the temperature of the stability transition from gypsum to anhydrite (around 43 °C e.g. Serafeimidis and Anagnostou (2015)) prevailed, which need to be accounted for when extrapolating the results to in-situ conditions. All porewater samples are close the equilibrium with regard to celestite, which is consistent with earlier studies for the Opalinus Clay from Mont Terri (Fernández et al., 2014; Wersin et al., 2022 and references within) and the Schlattingen borehole (Mazurek et al., 2015; Wersin et al., 2016). Although generally not detected by standard XRD measurements, Jenni et al. (2019) found indications for sub-μm celestite grains in two samples of the Opalinus Clay from the Schlattingen borehole by spectroscopic approaches. Within this general picture, a tendency for slight undersaturation (SQ) and oversaturation (AD) with regard to celestite is observed. In previous studies, the disturbance of the celestite equilibrium in borehole or squeezed waters was attributed to an increase in sulphate caused by the oxidation of pyrite (Fernández et al., 2014; Wersin et al., 2020). In the present study, this artefact likely did not occur, given the precautions taken to avoid oxidation and also due to the consistency of the SO_4/Cl ratio between AD and SQ samples (Fig. 4). On the contrary, Sr concentrations indicate a small but systematic shift to higher values in AD samples, exceeding the generally more dilute SQ aliquots (Fig. 5b), for which the reasons are not yet understood. Silica concentrations were only determined for AD samples and reflect quartz equilibrium.

4.3.2. *Calcite – dolomite equilibria and the effect of temperature*

For most samples, the SIs calculated for the experimental temperature of 25 °C, do not show a simultaneous equilibrium of the porewater with calcite and dolomite. If both minerals coexist in the clay rock, simultaneous equilibria should be attained under in-situ conditions and be reflected in the Ca^{2+}/Mg^{2+} activity ratio according to (Pearson et al., 2011)

$$log\left(\frac{a_{Ca^{2+}}}{a_{Mg^{2+}}}\right) = 2log\ K_{calcite} - log\ K_{dolomite} \quad (1)$$

Where K represents the equilibrium constant for the respective pure mineral phase. Fig. 8 visualizes the temperature dependency of this ratio based on thermodynamic data for calcite and dolomite (corresponding to ordered dolomite of the Nagra/PSI database) in the Thermoddem database (Blanc et al., 2012). Note that the slope and the position of this line might vary if the thermodynamic properties of dolomite in the rock deviate from the theoretical values or if solid solution effects become significant. If the Ca^{2+}/Mg^{2+} activity ratios of the AD and SQ samples

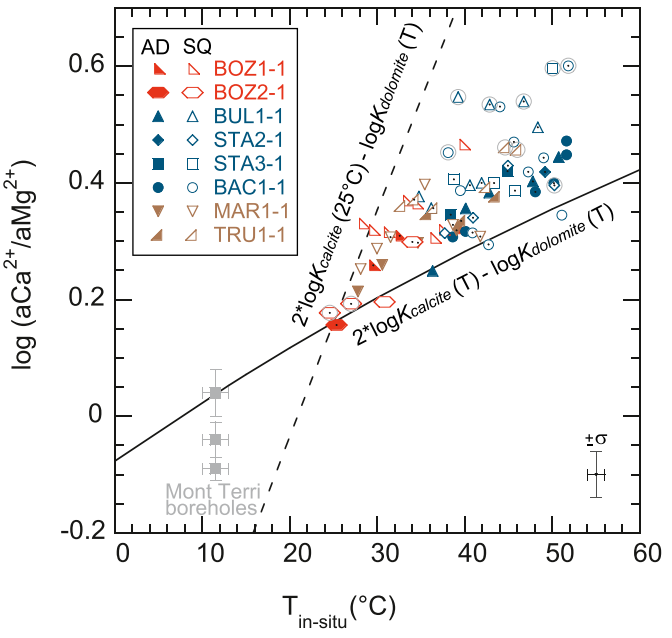

Fig. 8. Ca^{2+}/Mg^{2+} activity ratios vs. in-situ temperature as calculated with the Thermoddem database for AD and SQ samples from the Opalinus Clay and the confining units. The solid line indicates the aCa^{2+}/aMg^{2+} at coexisting calcite – dolomite equilibrium as a function of temperature according to eq 1, whereas the dashed line represents the aCa^{2+}/aMg^{2+} in case of fixed calcite equilibrium at 25 °C and dolomite equilibrium as a function of T. SQ samples with grey circles were obtained at ≥300 MPa, black dots indicate samples with dolomite/ankerite below detection limit. Note that for STA3-1 and BAC1-1 no in-situ T was determined and the temperature depth profile of the STA2-1 borehole was used instead.

are now plotted according to $T_{in\text{-}situ}$, two main observations are made: 1) the majority of the AD and SQ data fairly well follow the temperature dependence of the calcite – dolomite equilibrium, and 2) part of the samples, in particular from SQ experiments, deviate from the general trend and spread towards higher aCa^{2+}/aMg^{2+}. The first observation indicates that simultaneous calcite-dolomite equilibrium for the experimental temperature has not been attained. The measured aCa^{2+}/aMg^{2+} ratios rather reflect the ratio expected for calcite and dolomite equilibrium at the higher in-situ temperature of up to 50 °C, which may have been buffered against short term disturbances (temperature changes, disturbances of pCO_2) via the cation exchanger. Thus, in-situ temperatures increasing with depth may provide an explanation for i) the spread in the data e.g. between samples from the shallower JO boreholes and the deeper NL and ZNO boreholes and ii) for the difference of aCa^{2+}/aMg^{2+} ratios obtained in the present study in comparison with earlier data obtained from seepage waters of Mont Terri (Pearson et al., 2011) or Boom Clay at the Mol site (Wang et al., 2023). In the latter studies, in-situ temperatures of 13 and 16 °C, respectively prevailed and log aCa^{2+}/aMg^{2+} values between −0.2 and 0.04 were measured. The second observation, a spread towards higher aCa^{2+}/aMg^{2+} ratios, indicates for these samples an evolution of the porewaters towards equilibrium with calcite at colder (lab or cool storage) temperatures (calcite dissolution), whereas this is largely impeded for dolomite due to slower kinetics or the absence of notable amounts of dolomite (dashed line in Fig. 8). Note that SQ samples were generally processed after longer (cold-) storage compared with AD samples, which may explain an advanced evolution towards the new equilibrium state. Furthermore, some SQ samples were obtained by squeezing pressures ≥300 MPa and might therefore also be affected by pressure induced dissolution of calcite (Mazurek et al., 2015). To which degree the different quantity, timing and duration of CO_2 loss from AD and SQ samples, contributed to the observations remains unclear at present. Pearson et al. (2011) observed a positive correlation between the aCa^{2+}/aMg^{2+} ratios and the salinity of the seepage water in the three studied boreholes at Mont Terri. A direct dependency cannot not be confirmed with the present dataset.

4.3.3. *The pH/pCO_2 system*

The coupled pH/pCO_2 system is not only one of the most important parameters in geochemical systems as it controls the speciation, solubility and retention of various solutes as well as the stability of natural and engineered solid phases, it is also one of the most challenging to determine experimentally. Although AD and SQ experiments allow to directly determine pH and subsequently to constrain pCO_2 values by taking TIC or alkalinity into account, these data require a critical evaluation with respect to experimental artefacts and the changes from in-situ to laboratory conditions with respect to e.g. temperature.

The pH values measured for AD samples in-line (pH_{inline}) and on sample aliquots in the lab (pH_{lab}) span a range of 6.9–7.8 and 7.2–7.7, respectively, without any obvious trends with lithology, depth or regional setting. Despite the comparable ranges, a systematic shift towards lower pH_{inline} values compared with the corresponding pH_{lab} values was observed (pH_{inline}-pH_{lab} = avg ± 2·σ = -0.15 ± 0.48 pH units, Tables SI–4). Partial pressures of CO_2 calculated for the pH_{lab}/TIC and pH_{inline}/TIC datasets for a temperature of 25 °C vary between $10^{-2.6}$ and $10^{-1.4}$ bar, but remain in most cases below $10^{-1.8}$ bar (Fig. 9). The shift between in-line and lab pH and the oversaturation with respect to calcite (Fig. 7) indicate some outgassing of CO_2 during sampling, storage or measurement of the aliquots. Porewaters obtained by SQ are characterized by significantly higher pH values of 8.1–9.2, low CO_2 partial pressure of $10^{-3.1}$ to $10^{-4.6}$ bar (calculated with TIC for 25 °C) and, with one exception, a supersaturation with regard to calcite (SI > 1). These parameters indicate a stronger perturbation of the pH/pCO_2 system in the squeezed samples compared to AD, as has been observed previously within the Mont Terri project (Mazurek et al., 2017; Wersin et al., 2022) and to a lesser extent in the SQ study at the Schlattingen deep borehole (Mazurek et al., 2015). Generally, this has been attributed to outgassing of CO_2 during the squeezing process (Pearson et al., 2003; Wersin et al., 2022), but CO_2 loss during sample storage, preparation or pH

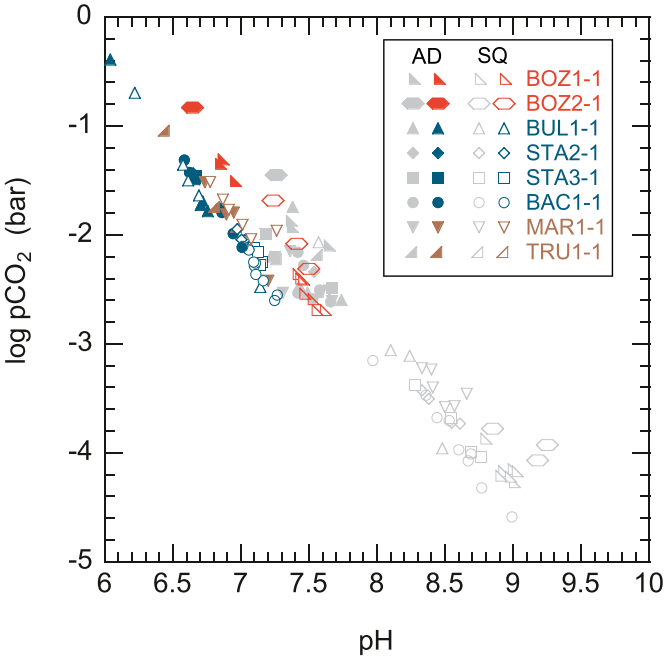

Fig. 9. pH and log pCO_2 in SQ (open) and AD samples (filled) for the Opalinus Clay and confining units as measured in the lab (grey) and after correcting for outgassing of CO_2 assuming calcite equilibrium (coloured).

measurement might contribute as well in case of aliquots with pCO_2 above atmospheric partial pressure (Pearson et al., 2011).

Thus, pH/pCO_2 values were corrected for a loss of CO_2 from the system by enforcing calcite saturation by addition of CO_2, a procedure analogous to that routinely applied to samples of deep groundwaters. Note that this approach results in slightly higher pCO_2 and lower pH values compared to a simple adjustment of pH to calcite equilibrium, as was for example applied by Fernández et al. (2014). Generally, after the correction a fair consistency in the AD and SQ datasets is obtained, with the exception of the samples from JO, where two distinct sample populations remain within the pH/pCO_2 relation (Fig. 9). The derived pH and pCO_2 values span, with few exceptions, a range of 6.6–7.6 and $10^{-1.4}$ to $10^{-2.7}$ bar, respectively. The AD samples largely plot at the lower pH (6.5–7) and higher pCO_2 ($10^{-1.3}$ to $10^{-2.1}$ bar) corner of the data field.

Such high pCO_2 values are above the range determined by pCO_2 measurements in the gas phase of rock samples from Mont Terri (Vinsot et al., 2008a), the Schlattingen borehole (Wersin et al., 2016), the Callovo-Oxfordian in the Paris Basin (Lassin et al., 2016; Vinsot et al., 2008b) or the Mol site (Honty et al., 2022). However, it is consistent with the range of pCO_2 values determined for expected in-situ temperatures of ~40–50 °C in sedimentary aquifers (Coudrain-Ribstein et al., 1998) or modelled under the assumption of pH control by different silicate mineral pairs for a temperature of 50 °C for an Opalinus Clay porewater of the Schlattingen borehole (Wersin et al., 2020 and references therein) and the ZNO-NL area (Mäder and Wersin, 2023). As discussed by e.g. Pearson et al. (2011) and Gaucher et al. (2009) silicate mineral reactions, namely of kaolinite, illite and chlorite, may exert an important control on the pH in clay rocks, but exhibit slow reaction kinetics. It may thus be envisioned that the low pH/high pCO_2 derived here reflects a not yet attained silicate mineral equilibrium for the laboratory temperatures.

Disturbances of the pCO_2/pH system may be also linked to microbial processes, which, depending on the microbial community and processes may increase or decrease the pCO_2 (Mijnendonckx et al., 2019). In the present study, anaerobic respiration of organic matter leading to an increase in pCO2 can be suspected for three AD samples and one SQ sample outside of the main sample group. The oxidation of pyrite and subsequent acidification and calcite dissolution can however be dismissed based on the stable SO_4/Cl ratios (4.2).

Despite the rather large uncertainty remaining with these highly reactive parameters, little variation of the other parameters is observed, due to the high buffering capacity of clay-rich rocks and the resulting insensitivity of the major-ion composition to pCO_2/pH (Pearson et al., 2011).

4.4. Porewater modelling

Geochemical modelling of porewaters in clay rocks is well established and has been successfully applied to Opalinus Clay (e.g. Pearson et al., 2003; Pearson et al., 2011; Wersin et al., 2016; Wersin et al., 2020 and references therein) and to other clay rocks, such as the Callovo-Oxfordian Formation (Gaucher et al., 2009) and the Boom Clay (De Craen et al., 2004b; Wang et al., 2023). The principle is to constrain the components of the pore solution with a set of mineral equilibria and cation exchange reactions according to Gibbs' phase rule, besides fixing conservative components not controlled by mineral reactions, such as chloride. Depending on the purpose of the modelling, these calculations may consider laboratory or in-situ conditions in particular with respect to temperature. Calculations at laboratory conditions are generally the first step when interpreting laboratory experiments or designing artificial porewaters for experiments. Calculations referring to in-situ conditions on the other hand are required when interpreting samples from borehole waters or when deriving porewater compositions for the prediction of radionuclide solubilities and speciation. Here, thermodynamic data at standard conditions are applied (25 °C, 1 bar) because the main purpose of the modelling is the comparison of the cation compositions of AD and SQ porewaters with cation occupancies from cation exchange experiments determined in the laboratory.

The concentrations of cations in porewaters are assumed to be constrained by the exchanger composition, thus by the exchangeable cations, present in much higher concentrations than those in dissolved form when normalised to the volume of porewater (Tournassat et al., 2015). For the model presented here the cation exchange capacity and exchanger composition was obtained from the independent dataset of cation exchange measurements via Ni-en extraction on material adjacent to AD core samples (Marques Fernandes et al., 2023). The relative occupancies of the different cations on the exchanger from these Ni-en extracts are derived by correcting the measured extracted cations for the contribution of dissolved salts. In practical terms, this was done by attributing extracted Cl to Na and extracted SO_4 to Ca (Marques Fernandes et al., 2023). The cation exchange model and selectivity coefficients used in the calculations were based on Pearson et al. (2011) (Supporting Information, Tables SI–5). Calcite, omnipresent in the considered formations, and celestite (both minerals exhibit rapid dissolution/precipitation kinetics) were assumed to be in equilibrium with the porewaters (section 4.3.1). On the other hand, dolomite equilibrium was not considered although this mineral is present in most considered lithologies, because of its sluggish kinetics and the indications of dis-equilibrium with regard to this phase in the cores cooled down to ambient temperatures for which the model is applied (see section 4.3.2). Moreover, gypsum equilibrium was assumed for the BUL1-1 borehole in which sulphate concentrations in the porewaters of the Opalinus Clay and confining units comply with an equilibrium assumption with regard to this phase.

One uncertainty pertains to the constraints on the pH/pCO_2 system in such clayrock systems. In general, two different approaches have been proposed: (i) adding a set of selected clay mineral equilibria to the geochemical model (Gaucher et al., 2009; Pearson et al., 2011) or (ii) fixing the pCO_2 (usually at −2.2 log (bar) in the case of Opalinus Clay) based on expert judgement (Mäder, 2009; Mäder and Wersin, 2023; Pearson et al., 2003; Wersin et al., 2016). Both approaches are disputable (Wersin et al., 2017). In the approach including clay mineral equilibria, uncertainties related to the thermodynamic data of clay minerals (e.g.Blanc et al., 2015) and conceptual issues regarding the thermodynamic stability of smectite and illite persist (Essene and Peacor, 1995; Lippmann, 1982). Moreover, it should be noted that the precise chemical composition of the clay minerals (illite, illite/smectite, kaolinite, chlorite) is not known for the Opalinus Clay or the confining units and that the limited time over which the samples were held at the experimental temperature of 25 °C, may not allow for clay minerals to participate in the fixation of the pH/pCO_2 system due to kinetic reasons (4.3.3). The second approach is primarily based on pCO_2 measurements from Opalinus Clay and other clay rocks, such as the Callovo-Oxfordian Formation and the Boom Clay (Gaucher et al., 2010; Honty et al., 2022; Lassin et al., 2016; Pearson et al., 2003; Wersin et al., 2016). It can be considered representative for a temperature range encountered in the low temperature environments as those in underground research laboratories or surface laboratories (10–25 °C) and is adopted here.

In principle, with the known exchanger composition, the considered mineral equilibria and the fixing of pCO_2, the system of major ions in the porewaters is entirely constrained according to the phase rule (Table 2). However, because of the uncertain Sr occupancy on the exchanger due to dissolution of celestite and possibly other minerals during Ni-en extraction (Wersin et al., 2020, see also Figs. SI–1), its concentration cannot be reliably determined and the Sr–SO_4 system remains underconstrained (except in the case of the additional constraint of gypsum equilibrium). Sulphate concentrations in porewater depend on the one hand on equilibrium with celestite and on the other hand on diffusive exchange with the bounding aquifers (Wersin et al., 2018, 2020) (sections 4.2.1; 4.3.1). The latter process, in turn, is dependent on the local hydrogeological conditions of the site. To overcome this general

Table 2
Constraints on component concentrations used for the three siting areas ZNO, NL and JO (see text).

Component	ZNO + JO	NL without BUL1-1	NL BUL1-1
	Constraint on component concentration		
Cl	fixed	fixed	fixed
SO_4	celestite	empirical relationship[a)]	gypsum
$CO_{3,t}$	fixed $pCO_2 = 10^{-2.2}$	fixed $pCO_2 = 10^{-2.2}$	fixed $pCO_2 = 10^{-2.2}$
pH	calcite	calcite	calcite
Na	fixed exchanger	fixed exchanger	fixed exchanger
K	fixed exchanger	fixed exchanger	fixed exchanger
Ca	fixed exchanger	fixed exchanger	fixed exchanger
Mg	fixed exchanger	fixed exchanger	fixed exchanger
Sr	empirical relationship[a)]	celestite	celestite

[a)] Relationship detailed in Supporting Information Figure SI-2.

uncertainty, AD and SQ data were evaluated separately for the three study areas in order to explore possible dependencies between relative depths, SO_4/Cl ratios and exchangeable Sr. The goal was to constrain either SO_4 or Sr with simple empirical relationships. Thus, for all three study areas, area-specific relationships could be derived as detailed in the SI (Figs. SI–2), except for the BUL1-1 case where the system was constrained by gypsum equilibrium. It should be noted that by adopting this procedure, a slight inconsistency was introduced since Sr–SO_4 constrained in this way was based on AD and in particularly SQ data, which ideally should be modelled from independent datasets.

Selected pairs of AD/SQ samples were modelled with PHREEQC and the PSI/Nagra database 2012 at 25 °C using the corresponding Cl concentrations of these experiments as input variable. Note that for the SQ experiments, for which no Ni-en extraction tests were carried out, the same exchanger composition as that from the nearby AD core was assumed. Examples of modelled results and their comparison with the measured AD and SQ data are shown as Schoeller plots in the SI (Figs. SI–3). In general, the match between modelled and measured data is satisfactory as illustrated in Fig. 10. Thus, for Opalinus Clay the agreement for the major ions Na, Ca, Mg, K and SO_4 as well as for Sr is within 50% (For Cl, the same concentrations as measured were considered). The larger deviation of the TIC concentrations in AD, reflects the lower pCO_2 selected in the model compared with the corrected pCO_2 values for AD experiments (Fig. 9) and may relate to the not yet attained silicate equilibria at the experimental temperature during the limited experimental timeframe (section 4.3.3). For the confining units (D.A.O. and Lias), the agreement between modelled and measured data is also within 50% for most cases, but variations are generally somewhat larger than for Opalinus Clay. A closer look at the data indicates a slight overprediction of the Ca and Mg levels compared to the AD/SQ data for most of the Opalinus Clay samples (in case of the BAC1-1 SQ samples the reverse is noted). The difference between modelled and measured data for divalent cations is somewhat more pronounced in the case of the confining units. The reason for this deviation is not clear. It might be related to potentially inaccurate selectivity coefficients in the cation exchange model or to the metastable conditions of the carbonate system upon changing temperature conditions (section 4.3.2).

This modelling exercise underlines the importance of taking the in-situ temperature and storage/extraction history of samples into account when interpreting pH and pCO_2 related parameters. Other major components appear much less affected due to the buffering capacity of the cation exchanger and the weak temperature dependency of the log-K constants of controlling mineral phases. This also applies to the transfer of data from 25 °C to the in-situ conditions, as recently shown by Mäder and Wersin (2023). Reference porewaters (used for safety analysis calculations) derived by those authors for the JO and NL/ZNO region for 25 °C and 50 °C showed only minor temperature dependency of the major ion composition within the temperature range of interest (40–50 °C). Somewhat larger changes were derived for pCO_2, which increased by 0.6–0.9 log (bar) and corresponding pH, which decreased by up to 0.5 units depending on the Al-silicate assemblage included. Wersin et al. (2020) already showed earlier that pressure effects on the porewater compositions of Opalinus Clay porewater at the in-situ depth can be expected to be very small.

5. Conclusions

A large set of AD and SQ experiments was conducted in the framework of Nagra's site investigation program, aiming at the determination of the free porewater composition in the clay-rich lithologies.

The two datasets obtained by these inherently different methods yield a consistent picture regarding the commonalities and differences between the three study areas, such as a significantly lower salinity in the JO area compared to NL and ZNO, or distinct gradients in salinity and porewater compositions with depth as controlled by the exchange with the adjacent aquifers. Moreover, ion ratios, which are important for the interpretation and modelling of the local porewater evolution, show a high degree of consistency and thus provide important and robust

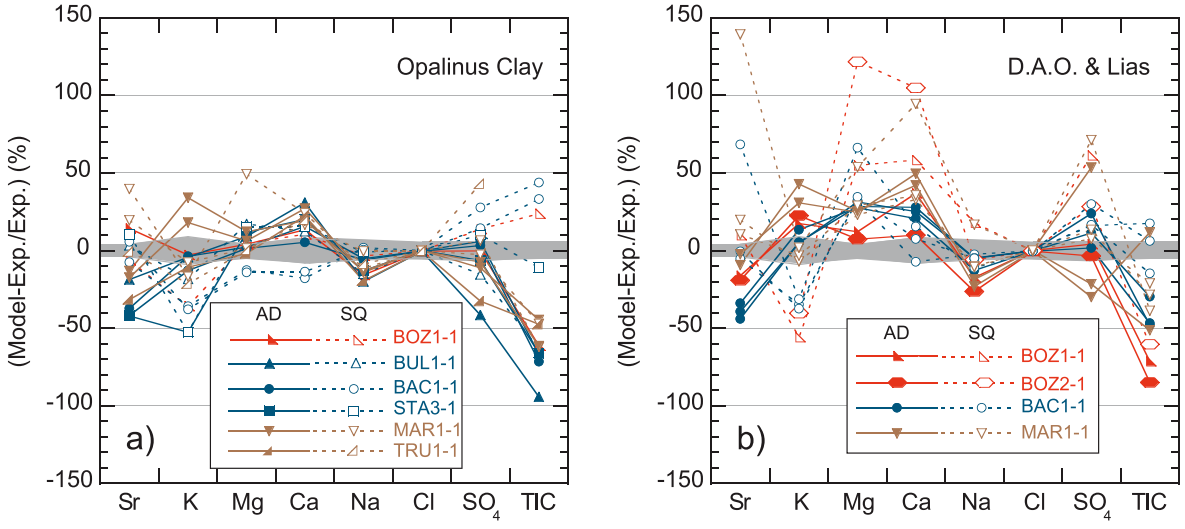

Fig. 10. Difference of the modelled ion concentrations to those determined experimentally for selected samples from the Opalinus Clay (a) and confining units (b). TIC refers to the corrected values as detailed in section 4.3.3. The grey shaded area indicates the analytical uncertainty.

anchor points for the interpretation of profiles of natural tracers. Internal controls on the porewater composition, such as equilibrium with minerals (e.g. celestite, gypsum in BUL1-1 and BAC1-1) and the cation exchanger population are similarly reflected in sample aliquots from both methods.

Besides these consistencies, a systematically lower salinity was obtained by SQ when compared to AD. The results of the present study indicate that SQ mobilizes a higher fraction of an anion depleted porewater, either because the higher flow velocity in SQ experiments shears more easily water close the clay surfaces, or due to the expulsion of water from interlayer (-like) pores due to their collapse in response to the squeezing pressure. This method related uncertainty tends to exceed the natural heterogeneity within the Opalinus Clay and confining units of the NL/ZNO study area, whereas it plays a subordinate role when considering the natural variability on a larger regional scale (JO vs. NL/ZNO). Hence, the SQ and AD method may be regarded complementary when aiming at a thorough investigation of the porewater composition and its natural variability in a regional context. The rather simple and established SQ method allows for the acquisition of a large data set, providing insights in the spatial variability. The more complex, labour intensive and rather unique AD method, on the other hand, may provide anchor points to further constrain the ionic strength of the free porewater, and may provide additional transport properties when extending percolation time.

For some parameters, in particular pH and pCO_2, method related artefacts were identified. Their influence on overall porewater composition is limited, but saturation indices of carbonate minerals can be shifted significantly. Attempts to correct for an obvious outgassing of CO_2 during the experiments yielded a reasonable consistent picture for both methods. Some discrepancies to earlier data suggest some remaining imprint of Al-silicate equilibria attained at higher in-situ temperatures. Due to the large dataset, a link could be made between Ca^{2+}/Mg^{2+} activity ratios and the in-situ temperature. It indicates that this ratio, which reflects the temperature dependent coexisting mineral equilibria of calcite and dolomite, may be buffered via the cation exchanger against short term disturbances, but tends to be overprinted by longer storage at temperatures differing from the in-situ temperature. Thus, the work highlights the importance of taking the temperature dependency of mineral equilibria and different mineral kinetics into account, when interpreting and modelling porewaters obtained in laboratory experiments under temperature conditions differing from in-situ. The redox conditions, one parameter of utmost importance with regard to radionuclide solubility and retardation, could not be determined by either method. Future research and method development is thus needed to allow porewater sampling as weakly disturbed by atmospheric oxygen as possible.

The good consistency between experimental data and the results of geochemical model calculations confirm the robustness of the geochemical model in predicting the major ion compositions for Opalinus Clay porewater, whereas some larger uncertainty remains for the clay-rich confining units. In turn, it underlines the suitability of AD and SQ samples as proxies for the in-situ porewaters, provided that redox, pH and pCO_2 are corrected for in-situ conditions by adequate model assumptions. Hence, with a combined approach of direct sampling methods, additional indirect methods such as cation exchange experiments and modelling efforts, methodological artefacts and conceptual uncertainties can be revealed and compensated for. This in turn allows for a more robust interpretation and assessment of the natural variability in terms of the past hydrogeochemical evolution as well as of the fate of radionuclides ultimately released into the system.

Declaration of competing interest

The authors declare that they have no known competing financial interests or personal relationships that could have appeared to influence the work reported in this paper.

Data availability

Data will be made available on request.

Acknowledgements

We thank P. Bähler and C. Pichler for contributing laboratory analyses, Th. Siegenthaler for trimming AD samples and supporting the AD lab, T. Oyama (CRIEPI, Japan) for performing the squeezing experiments, and the on-site and laboratory teams for sample preparation and processing. N. Schwendener (IRM, University of Bern) performed the X-ray CT scans of all AD samples. J.C. Robinet and M. Honty are thanked for their constructive and valuable reviews. Financial support by Nagra (National Cooperative for the Disposal of Radioactive Waste, Wettingen, Switzerland) is gratefully acknowledged.

Appendix A. Supplementary data

Supplementary data to this article can be found online at https://doi.org/10.1016/j.apgeochem.2023.105838.

References

Altmann, S., Tournassat, C., Goutelard, F., Parneix, J.-C., Gimmi, T., Maes, N., 2012. Diffusion-driven transport in clayrock formations. Appl. Geochem. 27, 463–478.

Aschwanden, L., Waber, H.N., Eichinger, F., Gimmi, T., 2023a. Isotope diffusive exchange experiments for deriving porewater isotope composition in low-permeability rocks – Improvements in experimental procedure and data processing. Appl. Geochem. 105844. https://doi.org/10.1016/j.apgeochem.2023.105844.

Aschwanden, L., Wersin, P., Debure, M., Traber, D., 2023b. Experimental study of water-extractable sulphate in Opalinus Clay and implications for deriving porewater concentrations. Appl. Geochem. 105837. https://doi.org/10.1016/j.apgeochem.2023.105837.

Blanc, P., Lassin, A., Piantone, P., Azaroual, M., Jacquemet, N., Fabbri, A., Gaucher, E.C., 2012. Thermoddem: a geochemical database focused on low temperature water/rock interactions and waste materials. Appl. Geochem. 27, 2107–2116.

Blanc, P., Vieillard, P., Gailhanou, H., Gaboreau, S., Gaucher, É., Fialips, C.I., Madé, B., Giffaut, E., 2015. A generalized model for predicting the thermodynamic properties of clay minerals. Am. J. Sci. 315, 734.

Coudrain-Ribstein, A., Gouze, P., de Marsily, G., 1998. Temperature-carbon dioxide partial pressure trends in confined aquifers. Chem. Geol. 145, 73–89.

De Craen, M., Van Geet, M., Wang, L., Put, M., 2004a. High sulphate concentrations in squeezed Boom Clay pore water: evidence of oxidation of clay cores. Phys. Chem. Earth, Parts A/B/C 29, 91–103.

De Craen, M., Wang, L., Van Geet, M., Moors, H., 2004b. The Geochemistry of Boom Clay Pore Water at the Mol Site, Status 2004. SCK•CEN Scientific Report, Mol, Belgium.

Essene, E.J., Peacor, D.R., 1995. Clay mineral thermometry—a critical perspective. Clay Clay Miner. 43, 540–553.

Falck, W.E., Bath, A.H., Hooker, P.J., 1990. Long-term solute migration profiles in clay sequences. Z. Dtsch. Geol. Ges. 141, 415–426.

Fernández, A.M., Sánchez-Ledesma, D.M., Tournassat, C., Melón, A., Gaucher, E.C., Astudillo, J., Vinsot, A., 2014. Applying the squeezing technique to highly consolidated clayrocks for pore water characterisation: lessons learned from experiments at the Mont Terri Rock Laboratory. Appl. Geochem. 49, 2–21.

Fernández, A.M., Villar, M.V., 2010. Geochemical behaviour of a bentonite barrier in the laboratory after up to 8years of heating and hydration. Appl. Geochem. 25, 809–824.

Gaucher, E., Lassin, A., Catherine, L., Fléhoc, C., Marty, N.C.M., Henry, B., Tournassat, C., Altmann, S., Vinsot, A., Buschaert, S., Matray, J., Leupin, O., De Craen, M., 2010. CO_2 partial pressure in clayrocks: a general model. In: Birkle, P., Torres-Alvarado, I. (Eds.), Water-Rock Interaction WRI-13. Taylor & Francis Group (CRC Press), Guanajuato, Mexico, pp. 855–858. Aug 2010. https://brgm.hal.science/hal-00664967.

Gaucher, E.C., Tournassat, C., Pearson, F.J., Blanc, P., Crouzet, C., Lerouge, C., Altmann, S., 2009. A robust model for pore-water chemistry of clayrock. Geochim. Cosmochim. Acta 73, 6470–6487.

Gimmi, T., Alt-Epping, P., 2018. Simulating Donnan equilibria based on the Nernst-Planck equation. Geochim. Cosmochim. Acta 232, 1–13.

Grambow, B., Landesman, C., Ribet, S., 2014. Nuclear waste disposal: I. Laboratory simulation of repository properties. Appl. Geochem. 49, 237–246.

Hanshaw, B.B., Coplen, T.B., 1973. Ultrafiltration by a compacted clay membrane—II. Sodium ion exclusion at various ionic strengths. Geochim. Cosmochim. Acta 37, 2311–2327.

Hedström, M., Karnland, O., 2011. Ca/Na selectivity coefficients from the Poisson–Boltzmann theory. Phys. Chem. Earth, Parts A/B/C 36, 1559–1563.

Honty, M., Frederickx, L., Wang, L., De Craen, M., Thomas, P., Moors, H., Jacops, E., 2022. Boom Clay pore water geochemistry at the Mol site: experimental data as determined by in situ sampling of the piezometers. Appl. Geochem. 136, 105156.

Horseman, S.T., Higgo, J.J.W., Alexander, J., Harrington, J.F., 1996. Water, Gas and Solute Movement through Argilaceous Media, OECD, Report CC-96/1. NEA, Paris.

Hsiao, Y.-W., Hedström, M., 2017. Swelling pressure in systems with Na-montmorillonite and neutral surfaces: a molecular dynamics study. J. Phys. Chem. C 121, 26414–26423.
Huclier-Markai, S., Landesman, C., Rogniaux, H., Monteau, F., Vinsot, A., Grambow, B., 2010. Non-disturbing characterization of natural organic matter (NOM) contained in clay rock pore water by mass spectrometry using electrospray and atmospheric pressure chemical ionization modes. Rapid Commun. Mass Spectrom. 24, 191–202.
Hummel, W., Thoenen, T., 2022. The PSI Chemical Thermodynamic Database 2020, Nagra Technical Report NTB 21-03. Wettingen, Switzerland.
Iyer, B.V., 1990. Pore water extraction - comparison of saturation extract and high-pressure squeezing. In: Hoddinott, K.B., Lamb, R.O. (Eds.), Physico-Chemical Aspects of Soil and Related Materials, pp. 159–170. https://doi.org/10.1520/STP1095-EB.
Jäckli, H., 1970. Kriterien zur Klassifikation von Grundwasservorkommen. Eclogae Geol. Helv. 63 https://doi.org/10.5169/seals-163850.
Jenni, A., Aschwanden, L., Lanari, P., de Haller, A., Wersin, P., 2019. Spectroscopic Investigation of Sulphur-containing Minerals in Opalinus Clay, Nagra Arbeitsbericht NAB 19-23. Nagra, Wettingen, Switzerland.
Kharaka, Y.K., Berry, F.A.P., 1973. Simultaneous flow of water and solutes through geological membranes—I. Experimental investigation. Geochim. Cosmochim. Acta 37, 2577–2603.
Kharaka, Y.K., Smalley, W.C., 1976. Flow of water and solutes through compacted clays. AAPG (Am. Assoc. Pet. Geol.) Bull. 60, 973–980.
Lassin, A., Marty, N.C.M., Gailhanou, H., Henry, B., Trémosa, J., Lerouge, C., Madé, B., Altmann, S., Gaucher, E.C., 2016. Equilibrium partial pressure of CO2 in Callovian–Oxfordian argillite as a function of relative humidity: experiments and modelling. Geochim. Cosmochim. Acta 186, 91–104.
Lerouge, C., Debure, M., Henry, B., Fernandez, A.-M., Blessing, M., Proust, E., Madé, B., Robinet, J.-C., 2020. Origin of dissolved gas (CO2, O2, N2, alkanes) in pore waters of a clay formation in the critical zone (Tégulines Clay, France). Appl. Geochem. 116, 104573.
Lippmann, F., 1982. The thermodynamic status of clay minerals. Dev. Sedimentol. 25, 475–485.
Mäder, U., 2009. Reference Pore Water for the Opalinus Clay and "Brown Dogger" for the Provisional Safety-Analysis in the Framework of the Sectorial Plan - Interim Results (SGT-ZE), Nagra Arbeitsbericht NAB 09-14. Nagra, Wettingen, Switzerland.
Mäder, U., 2018. Advective displacement method for the characterisation of pore water chemistry and transport properties in claystone. Geofluids 2018, 1–11.
Mäder, U., Waber, H.N., 2017a. Results of Advective Displacement/Multi-Component Transport Experiments from Claystone Samples of the Schlattingen Borehole, Nagra Arbeitsbericht NAB 17-16. Nagra, Wettingen, Switzerland.
Mäder, U., Waber, H.N., Gautschi, A., 2004. A new method for porewater extraction from claystone and determination of transport properties with results for Opalinus Clay (Switzerland). In: Wanty, R.B., Seal, R.R. (Eds.), 11th Internat. Symp. On Water-Rock Interaction - WRI-11 1. Taylor & Francis Group, pp. 445–449.
Mäder, U., Wersin, P., 2023. Reference Pore Waters for SGT3 of the Opalinus Clay for the Siting Regions Zürich Nordost (ZNO), Nördlich Lägern (NL) and Jura Ost (JO), Nagra Arbeitsbericht NAB 22-47. Nagra, Wettingen, Switzerland.
Mäder, U.K., Waber, H.N., 2017b. Characterization of pore water, ion transport and water-rock interaction in claystone by advective displacement experiments. Procedia Earth and Planetary Science 17, 917–920.
Madritsch, H., 2015. Outcrop-scale fracture systems in the Alpine foreland of central northern Switzerland: kinematics and tectonic context. Swiss J. Geosci. 108, 155–181.
Marques Fernandes, M., Mazurek, M., Wersin, P., Wüst, R., Baeyens, B., 2023. Cation-exchange properties of the Mesozoic sedimentary sequence of Northern Switzerland and modelling of the Opalinus Clay porewater. Appl. Geochem. 105852. https://doi.org/10.1016/j.apgeochem.2023.105852.
Mazurek, M., Al, T., Celejewski, M., 2017. Mont Terri DB-A Experiment: Comparison of Pore-Water Investigations Conducted by Several Research Groups on Core Materials from the BDB-1 Borehole. NWMO-TR–2017-09. Nuclear Waste Mangement Organization (NWMO), Toronto, Canada.
Mazurek, M., Gimmi, T., Zwahlen, C., Aschwanden, L., Gaucher, E.C., Kiczka, M., Rufer, D., Wersin, P., Marques Fernandes, M., Glaus, M., Van Loon, L.R., Traber, D., Schnellmann, M., Vietor, T., 2023. Swiss Deep Drilling Campaign 2019–2022: Geological overview and rock properties with focus on porosity and pore-space architecture. Appl. Geochem. 105839. https://doi:org/10.1016/j.apgeochem.2023.105839.
Mazurek, M., Oyama, T., Wersin, P., Alt-Epping, P., 2015. Pore-water squeezing from indurated shales. Chem. Geol. 400, 106–121.
Meunier, A., Velde, B., 2004. Illite. Origins, Evolution and Metamorphism. Springer Berlin, Heidelberg.
Mijnendonckx, K., Miroslav, H., Wang, L., Jacops, E., Provoost, A., Mysara, M., Wouters, K., De Craen, M., Leys, N., 2019. An active microbial community in Boom Clay pore water collected from piezometers impedes validating predictive modelling of ongoing geochemical processes. Appl. Geochem. 106, 149–160.
Muurinen, A., Carlsson, T., 2007. Development of methods for on-line measurements of chemical conditions in compacted bentonite. Phys. Chem. Earth, Parts A/B/C 32, 241–246.
Parkhurst, D.L., Appelo, C.A.J., 2013. Description of input and examples for PHREEQC version 3—a computer program for speciation, batch-reaction, one-dimensional transport, and inverse geochemical calculations. In: U.S. Geological Survey Techniques and Methods, p. 497 book 6, chap. A43, available only at. https://pubs.usgs.gov/tm/06/a43/.
Pearson, F., Arcos, D., Bath, A., Boisson, J., Fernández, A.M., Gäbler, H., Gaucher, E., Gautschi, A., Griffault, L., Hernán, P., 2003. Geochemistry of water in the Opalinus clay formation at the Mont Terri rock laboratory. Swiss Federal Office for Water and Geology Series 319.
Pearson, F.J., 1999. What is the porosity of a mudrock? Geological Society, London, Special Publications 158, 9–21.
Pearson, F.J., Tournassat, C., Gaucher, E.C., 2011. Biogeochemical processes in a clay formation in situ experiment: Part E – equilibrium controls on chemistry of pore water from the Opalinus Clay, Mont Terri Underground Research Laboratory, Switzerland. Appl. Geochem. 26, 990–1008.
RWI, 2020. SGT-E3 Deep Drilling Campaign (TBO): Experiment Procedures and Analytical Methods at RWI,. University of Bern. Nagra Arbeitsbericht NAB 20-13., Nagra, Wettingen, Switzerland.
Serafeimidis, K., Anagnostou, G., 2015. The solubilities and thermodynamic equilibrium of anhydrite and gypsum. Rock Mech. Rock Eng. 48, 15–31.
Sposito, G., 2004. The Surface Chemistry of Natural Particles. Oxford University Press on Demand.
Sun, Z., Wu, K., Shi, J., Zhang, T., Feng, D., Huang, L., Li, X., 2019. An analytical model for transport capacity of water confined in nanopores. Int. J. Heat Mass Tran. 138, 620–630.
Thoenen, T., Hummel, W., Berner, U., Curti, E., 2014. The PSI/Nagra chemical thermodynamic database 12/07. In: PSI Bericht, Report No.14–.04. https://www.dora.lib4ri.ch/psi/islandora/object/psi%3A29731.
Tournassat, C., Appelo, C.A.J., 2011. Modelling approaches for anion-exclusion in compacted Na-bentonite. Geochim. Cosmochim. Acta 75, 3698–3710.
Tournassat, C., Chapron, Y., Leroy, P., Bizi, M., Boulahya, F., 2009. Comparison of molecular dynamics simulations with triple layer and modified Gouy–Chapman models in a 0.1 M NaCl–montmorillonite system. J. Colloid Interface Sci. 339, 533–541.
Tournassat, C., Vinsot, A., Gaucher, E.C., Altmann, S., 2015. Chapter 3 - chemical conditions in clay-rocks. In: Tournassat, C., Steefel, C.I., Bourg, I.C., Bergaya, F. (Eds.), Developments in Clay Science. Elsevier, pp. 71–100.
Vinsot, A., Appelo, C.A.J., Cailteau, C., Wechner, S., Pironon, J., De Donato, P., De Cannière, P., Mettler, S., Wersin, P., Gäbler, H.E., 2008a. CO2 data on gas and pore water sampled in situ in the Opalinus Clay at the Mont Terri rock laboratory. Phys. Chem. Earth, Parts A/B/C 33, S54–S60.
Vinsot, A., Mettler, S., Wechner, S., 2008b. In situ characterization of the Callovo-Oxfordian pore water composition. Phys. Chem. Earth, Parts A/B/C 33, S75–S86.
Wang, L., Honty, M., De, C., Frederickx, L., 2023. Boom Clay pore-water geochemistry at the Mol site: chemical equilibrium constraints on the concentrations of major elements. Appl. Geochem. 148, 105541.
Wersin, P., Gimmi, T., Ma, J., Mazurek, M., Zwahlen, C., Aschwanden, L., Gaucher, E.C., Traber, D., 2023. Porewater profiles of Cl and Br in boreholes penetrating the Mesozoic sequence in northern Switzerland. Appl. Geochem. 105845. https://doi.org/10.1016/j.apgeochem.2023.105845.
Wersin, P., Gimmi, T., Mazurek, M., Alt-Epping, P., Pękala, M., Traber, D., 2018. Multicomponent diffusion in a 280 m thick argillaceous rock sequence. Appl. Geochem. 95, 110–123.
Wersin, P., Mazurek, M., Gimmi, T., 2022. Porewater chemistry of Opalinus clay revisited: findings from 25 years of data collection at the Mont Terri rock laboratory. Appl. Geochem. 138, 105234.
Wersin, P., Mazurek, M., Mader, U.K., Gimmi, T., Rufer, D., Lerouge, C., Traber, D., 2016. Constraining porewater chemistry in a 250 m thick argillaceous rock sequence. Chem. Geol. 434, 43–61.
Wersin, P., Pekala, M., Mazurek, M., Gimmi, T., Mäder, U., Jenni, A., Rufer, D., Aschwanden, L., 2020. In: Porewater chemistry of Opalinus clay: methods, data, modelling & buffering capacity. NagraTechnical Report NTB 18-01. Nagra, Wettingen, Switzerland.
Wersin, P., Traber, D., Mäder, U.K., Mazurek, M., Waber, H.N., Rufer, D., Gimmi, T., Cloet, V., 2017. Porewater chemistry in claystones in the context of radioactive waste disposal. Procedia Earth and Planetary Science 17, 718–721.
Zwahlen, C., Gimmi, T., Jenni, A., Kiczka, M., Mazurek, M., Van Loon, L.R., Mäder, U., Traber, D., 2023. Chloride accessible porosity fractions across the Jurassic sedimentary rocks of northern Switzerland. Appl. Geochem. 105841. https://doi.org/10.1016/j.apgeochem.2023.105841.